

# S-BUN: Soft Bifunctional Utility Module for Robot Sensing and Signaling

Suksakaow Mahuttanatan<sup>1,‡</sup>, Naris Asawalertsak<sup>1,‡</sup>, Jinjuta Paripurana<sup>1</sup>, Kanut Tarapongnivat<sup>1</sup>,  
Thirawat Chuthong<sup>1</sup>, and Poramate Manoonpong<sup>1,2,\*</sup>, *Senior Member, IEEE*

**Abstract**—Conventional approaches in robotics for perceiving the environment and signaling the robot’s state or intention for human-robot interaction involve the use of separate sensing and signaling systems. This can sometimes result in high costs and complex system installations. In this study, we propose an alternative approach, integrating both robot sensing and signaling mechanisms into a single utility module (called S-BUN, Soft Bifunctional Utility module for robot sensing and signaling). Soft material (Ecoflex 00-10 silicone) is used to form its bun-like structure with a central cavity filled with a NaCl solution. Inspired by honeycombs, the module’s surface incorporates a hexagonal pattern to enhance structural robustness. The design of S-BUN enables it to function as a sensor for both non-contact proximity and touch sensing, utilizing the NaCl solution. Additionally, it serves as a signaling mechanism to indicate the robot’s state through the active inflation and deflation dynamics of the module, simulating lifelike breathing patterns. Through our experiments, we present S-BUN’s capabilities in proximity and touch sensing, including its ability to discern various touch intensities. Finally, we demonstrate the application of S-BUN in the context of reactive behavioral control for a crawling robot and human-robot interaction scenarios.

**Index Terms**—Robot Perception, Soft Sensors, Bio-inspired Design, Hexagonal Pattern, Capacitive Sensing, Robotic Breathing Mechanism

## I. INTRODUCTION

Sensing is a critical feature of robots, enabling them to perceive and interact with their surroundings effectively. As the field of robotics has advanced, the limitations of traditional perception methods, primarily relying on rigid materials (like metals or semiconductors) along with their specific functionalities, have become increasingly apparent [2]. For example, conventional (rigid) touch sensors, while reliable in controlled settings, are inflexible and often lack a sense of softness for soft human-robot interaction [3], [4].

To address this shortcoming, there has been a growing interest in the development of soft touch sensors [2]. In response, the field of materials science has played a pivotal role in advancing soft touch sensor technology. One area of exploration is the use of conductive threads, which show promise for creating flexible, textile-based soft touch sensors [5]. These threads are valued for their adaptability; however,

<sup>‡</sup>These authors contributed equally to this work.

<sup>1</sup>S.M., N.A., K.T., T.C. and P.M. are with the Bio-inspired Robotics and Neural Engineering Laboratory, School of Information Science and Technology, Vidyasirimedhi Institute of Science and Technology, Rayong, Thailand.

<sup>2</sup>P.M. is also with the Embodied Artificial Intelligence and Neurorobotics Laboratory, SDU Biorobotics, the Mærsk Mc-Kinney Møller Institute, University of Southern Denmark, Odense, Denmark. (\*Corresponding author; e-mail: poramate.m@vistec.ac.th)

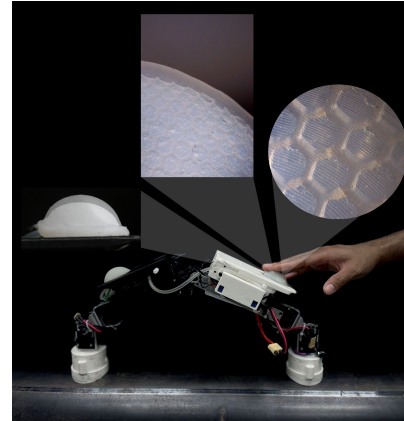


Fig. 1: S-BUN installed on an inchworm-inspired crawling robot (iCrawl) [1]. It is used for reactive behavioral control of the robot, enabling the robot to react to human touch. Additionally, it can signal the robot’s state through its breathing motion (see [www.manoonpong.com/SBUN/video.mp4](http://www.manoonpong.com/SBUN/video.mp4)). Three inset images expand the dynamics of S-BUN and provide magnified views of the hexagonal pattern on the surface of S-BUN. The left inset shows the inflation and deflation dynamics (breathing) of S-BUN, increasing in height during the inflation phase and decreasing in height during the deflation phase. The middle inset shows a zoomed view of the pattern at the edge, illustrating the pattern size concerning the overall S-BUN size. The right inset shows the detailed hexagonal pattern of the silicone.

they face limitations in terms of stretchability. Unlike other elastic materials, such as silicone, conductive threads have a restricted capacity to stretch. Stretching them beyond a certain point can compromise their conductivity, leading to increased resistance or even breakage. This limitation is a significant concern, particularly in applications requiring high elasticity.

An alternative approach relies on carbon materials, known for their conductive properties. They have also been utilized in soft touch sensor development, particularly for detecting changes in pressure [6], [7], [8]. However, these materials face their own set of challenges. One significant issue is their sensitivity to environmental noise, which can result in the detection of unintended signals, especially in variable and unpredictable settings [9]. Additionally, their long-term stability is at risk when exposed to certain chemicals or high humidity, leading to drifts in sensor readings over time [10].

One of the most advanced soft touch sensors is electronic skin (e-skin), inspired by human skin [11]. It is based on a semiconducting polymer-based material and can perform multimodal sensing, detecting temperature variations and a wide range of pressures ranging from gentle to strong touches. Additionally, it is also flexible and stretchable, en-

abling attachment to the human body [2] or soft robots [12]. However, while these soft sensors demonstrate advanced features in terms of flexibility, adaptability, and versatility, they typically function solely as a sensing system and lack the functionality to signal or indicate the state of the systems or robots.

Recognizing that while sensing is crucial, understanding the robot's state is equally important as another dimension for human-robot communication, interaction, and even anticipation [13], [14]. From this point of view, besides conventional signaling mechanisms, pneumatically actuated soft robotics technology has recently been employed to create signaling systems for transmitting robot information to humans as nonverbal communication [15], [16], [17]. For instance, [15] developed a pneumatically actuated soft robotic sleeve (called WISARD or Weight Informing Soft Artificial Robotic Dermis) and applied it to a traditional robot arm. The soft sleeve emulates tensed muscles, enabling humans to anticipate the approximate object weight lifted by the arm. This soft nonverbal signaling mechanism can facilitate nonverbal robot-human interaction during a handover task. A biomorphic soft robotic skin (called BioMORF) is introduced for a hexapod robot in [16] The skin with respiratory-like motions (breathing) can increase the biomorphic characteristics of the robot and enable nonverbal human-robot communication. While this soft robotics technology can indicate the robot's state, it has not yet been integrated with a sensing mechanism.

From this perspective, we propose here for the first time the Soft Bifunctional Utility Module for Robot Sensing and Signaling (S-BUN, Fig. 1). It integrates a soft (touch) sensing system and a soft (nonverbal) signaling system [16] into a single versatile system or module. The special design of S-BUN leads to both non-contact proximity and touch sensing, utilizing a NaCl solution. The NaCl solution is preferred over other media, such as foam, due to its conductive and flexible properties. This conductive medium enhances the module's capacity to detect touch and proximity by altering the electric charge distribution. Consequently, the module can respond to human interaction, including proximity sensing without physical contact. As an object, like a human hand, approaches S-BUN, its presence induces changes in the electric charge distribution across the air gap, enabling proximity detection. S-BUN also serves as a signaling mechanism through the active inflation and deflation dynamics of the module, simulating breathing patterns. The breathing patterns are designed to enhance human-robot interaction by creating a more lifelike appearance, focusing on nonverbal communication and engagement rather than augmenting the sensing capabilities of S-BUN. The module surface integrates a honeycomb-inspired hexagonal pattern. This pattern, known for its high strength, shear rigidity, and excellent energy absorption, enhances the module's stretchability and durability [18], [19], [20]. The hexagonal structures are made from the same silicone material as the S-BUN skin, molded with an indented pattern to maximize air inflation ability while ensuring durability through a thicker hexagonal design.

S-BUN is designed to address current challenges, including the high cost, complexity, single-function limitations, and lack of versatility and adaptability/scalability, as follows:

- **Cost-effectiveness and simplicity:** It addresses the financial and operational barriers often associated with advanced robotic sensor systems. By being affordable, simple, and straightforward to use, S-BUN makes sensing technology more accessible and practical for a diverse range of users and applications.
- **Multifunction:** It serves as a touch sensor, proximity sensor, and robot state indicator<sup>1</sup>. This multifunctionality directly tackles the issue of single-function sensors, providing a more comprehensive sensing solution. This enhances the robot's ability to interact with and understand its environment in a more integrated and nuanced manner.
- **Scalable design:** The scalability of S-BUN to various robotic platforms, from small wearable devices to larger industrial robots, addresses the need for versatile and scalable sensors. This scalability ensures that the technology can be effectively utilized in a wide range of contexts and applications.

## II. MATERIAL METHODS

### A. S-BUN System Overview

This study focuses on designing and implementing a versatile module to enhance both robot perception and state indication during close human-robot interaction. This effort has led to our Soft Bifunctional Utility Module for Robot Sensing and Signaling (S-BUN), consisting of three primary components: i) a pneumatically soft actuator with a conductive solution (referred to as a multi-functional soft module), ii) an air regulation system, and iii) an electronic circuit (Fig. 2). Each of these components is described in detail below.

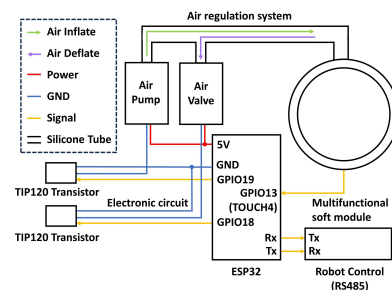


Fig. 2: The S-BUN system comprises three main components. The first is a multi-functional soft module made of silicone with a hexagonal surface design to ensure soft and robust expandability for our signaling mechanism. This module is infused with a NaCl solution to provide electrical conductivity for our sensing mechanism. The second component is an air regulation system equipped with a pump and valve responsible for the inflation and deflation mechanism of the soft module. The final component is an electronic circuit built around the core ESP32 board.

<sup>1</sup>In this study, 'state' specifically refers to basic robot situations, including standing, crawling, and stopping, as these are the states tested.

1) *Multifunctional Soft Module*: Constructed from Ecoflex 00-10 silicone, the module serves as the primary interface for non-contact proximity and touch interactions. It is embedded with a NaCl solution, specifically chosen for its proficiency in proximity and touch sensing. The module design includes an air pocket that can either inflate or deflate, simulating a breathing function. This function can be utilized for signaling or indicating the robot's state. Figure 2 shows how the soft module part connects to the air regulation system. The figure also depicts the direction of airflow for inflation and deflation (robot breathing-based state indication), managed by the air pump and valve. The output signals from the GPIO points (GPIO18 and GPIO19) of the ESP32 board are transmitted to control the air pump and valve for the breathing function. The output pin of the soft module is connected to a capacitive touch sensor pin (GPIO13) on the ESP32 board for proximity and touch sensing.

2) *Air Regulation System*: It consists of an air pump and air valve, crucial for managing the inflation and deflation of the soft module. The airflow directions (Fig. 2) support the module's unique "breathing" characteristic, which can act as a robot state indicator, enhancing its adaptability to different interaction scenarios.

3) *Electronic Circuit*: The circuit includes the ESP32 board and transistors (Fig. 2) to detect non-contact proximity and touch information and generate output signals for robot breathing as well as robot reactive behavioral control. When an object (e.g., a human hand) approaches or makes contact with the module, it receives information through the NaCl solution and the capacitive touch sensor channel of the ESP32. The capacitive-based proximity/touch sensing information is further pre-processed using a low-pass filter before being transmitted to control the robot over serial communication (RS485), enabling it to respond to the feedback. For instance, if the robot is touched through the soft module, it can react by halting to prevent injury to humans or potential damage (see the Experiments and Results section). Additionally, we can program the ESP32 board to control the air regulation system, regulating the breathing motion of the soft module to indicate the robot's state (see the Experiments and Results section).

### B. Multifunctional Soft Module Design

Among the components of S-BUN described above, a key contribution of our study is the design of the soft module. This module consists of three key elements (Fig. 3a): i) a soft sandwich part (skin with outer and inner layers filled with a NaCl solution between the layers) for non-contact proximity and touch sensing, ii) a base part for the installation of the module on a robot, and iii) a cavity part for simulating breathing through the inflation and deflation of air.

To attain non-contact proximity and touch sensitivity, it is necessary to determine the skin layer thickness ( $t$ , Fig. 3a) of the soft module. It is an important design parameter that affects the capacitive sensing performance of the soft module. To investigate this, we evaluated the capacitive sensing

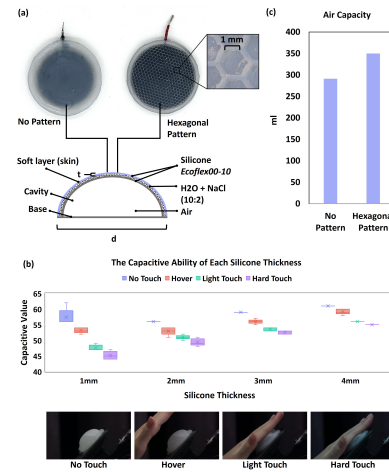


Fig. 3: S-BUN with a hexagonal surface pattern and without any pattern. (a) A graphical representation illustrates the structure and section of the soft module of S-BUN, highlighting " $t$ " as the thickness of the upper silicone layer with the hexagonal pattern and " $d$ " as the module's diameter. (b) A comparison of the capacitive sensing across different silicone thickness levels ( $t = 1$  mm, 2 mm, 3 mm, and 4 mm) under different conditions, including no touch, hover, light touch (pressed for 1 newton using a force gauge), and hard touch (pressed for 5 newtons using a force gauge). It should be noted that for the test, S-BUN has a diameter of  $d = 50$  mm. (c) A comparison of the air capacity, in milliliters, for the module with a hexagonal pattern (structured surface) and without the pattern (flat surface), emphasizing the enhanced performance of the hexagonal surface design. It should be noted that for the test, the sizes of the S-BUN parameters are  $d = 50$  mm and  $t = 1$  mm.

characteristics at different thickness levels (1 mm, 2 mm, 3 mm, and 4 mm) under various conditions (no touch, hover (non-contact proximity sensing), light touch (low-pressure sensing), and hard touch (high-pressure sensing)). The result in Fig. 3b shows that the 1 mm silicone layer displayed significantly different capacitive values between no touch and touch conditions, particularly when compared to the thick one (4 mm variant). The improved performance of the thinner layer leads to decreased signal attenuation, a denser concentration of capacitive elements within the material, and a quicker response time. Accordingly, we designed our soft module with a layer thickness of 1 mm.

However, with the thin layer, the skin can be easily broken after some cycles of inflation and deflation. Consequently, we applied a honeycomb-inspired hexagonal pattern (Fig. 3a) to the S-BUN's skin (or surface). Hexagons, with their six equal sides (each measuring 1 mm in length), ensure uniform stress and strain distribution, leading to resilience and durability. This geometric design not only adds an aesthetic dimension to the soft module but also bolsters its structural integrity, as demonstrated in (Fig. 3c). Under a 5 LPM capacity air pump, the structure with no pattern could withstand the air pressure for 35 seconds, equivalent to approximately 290 millimeters of air (Fig. 3c), before breaking. In contrast, the hexagonal-patterned structure exhibited superior endurance, enduring the air pressure for 42 seconds, equivalent to approximately 350 millimeters of air (Fig. 3c), before breaking. The increase of 58 milliliters, or approximately 20 percent, in capacity observed in the hexagon-patterned structure empha-

sizes the role of the hexagon in fortifying material robustness and making it more resilient to mechanical stresses. It is important to note that S-BUN's capacity was not measured directly but inferred from air pump readings to demonstrate the hexagon pattern's benefits. This resilience is especially crucial in robotic applications involving dynamic motions (i.e., breathing function) and varying pressures, positioning the hexagon pattern as the preferred choice for the S-BUN skin.

### III. EXPERIMENTS AND RESULTS

This section presents the four main experiments conducted to assess the performance of S-BUN. The first experiment investigated the expansion dynamics (signaling) of S-BUN and its sensing response during breathing motions. The second experiment examined the scalability of S-BUN at various sizes and their sensing responses. The third experiment evaluated the sensing performance and cost-effectiveness of S-BUN across several conductive materials. Finally, we demonstrated the use of S-BUN for reactive robot behavioral control and human-robot interaction.

#### A. Experiment 1: S-BUN Expansion Dynamics

In addition to the sensing capabilities of S-BUN, it was integrated with a signaling mechanism utilizing a robotic breathing mechanism, which operates based on expansion dynamics through inflation and deflation. Breathing, a natural and organic process, imbues robots with a more lifelike and relatable presence. This humanization of robots can enhance trust and improve soft human-robot interaction [14], [16]. S-BUN's ability to inflate and deflate allowed it to mimic a rhythmic breathing pattern, adding to its lifelike qualities (Fig. 4). S-BUN was programmed with a breathing (inflation and deflation) cycle at a frequency of approximately 11 beats per minute (BPM)<sup>2</sup>. The cycle was designed based on the frequency range of a soft robot's breathing (7–12.5 BMP), potentially influencing human perceptions of effective human-robot interaction as suggested by [14], [16].

Figure 4a illustrates the inflation and deflation dynamics of S-BUN, emphasizing the increase in height ( $H_1 = 20$  mm) during Phase I (inflation), the reduction in height ( $H_2 = 15$  mm) during Phase II (deflation), and the maintenance of the  $H_2$  height during Phase III (stabilization). This three-phase breathing cycle was efficiently managed by the synchronized functioning of a single pump and valve. Figure 4b presents the on/off (1/0) status of the pump and valve during the 10-second inflate/deflate cycle, demonstrating the specific on/off pattern of the pump and valve in each stage. The pump was engaged to fill the structure with air, inflating S-BUN, while the valve remained closed to keep the air inside. During deflation, the pump was turned off, and the valve opened to let the air out. Both the pump and valve were inactive during the stabilization phase, keeping S-BUN's height at  $H_2$ .

<sup>2</sup>11 BPM can be translated to a pattern of 1.5 s for inflation, 2 s for deflation, and a 2-s stabilization, closely mirroring typical human breathing patterns.

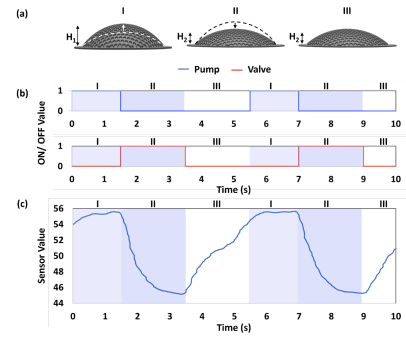


Fig. 4: Expansion dynamics of S-BUN as a signaling mechanism. (a) S-BUN during inflation and deflation, highlighting the increase in height ( $H_1$ ) during Phase I (inflation), the decrease in height ( $H_2$ ) during Phase II (deflation), and the maintenance of the  $H_2$  height during Phase III (stabilization). (b) The on/off (1/0) status of the pump and valve during the 10-second inflate/deflate cycle. (c) A sine wave pattern of the S-BUN sensing value throughout the breathing cycle under normal conditions (no touch). It should be noted that for the test, S-BUN has a diameter of  $d = 50$  mm and a thickness of  $t = 1$  mm.

Figure 4c illustrates the capacitive readings of S-BUN during the breathing cycle. S-BUN exhibited a capacitive sensing response resembling a sine wave pattern following the breathing cycle, displaying higher values during the inflation phase and a decrease during deflation, followed by a rise during the stabilization phase. This waveform, with a frequency of 0.18 Hz, effectively demonstrates S-BUN's consistent ability to reliably detect and respond to its state of expansion or contraction.

#### B. Experiment 2: S-BUN Scalability

Although, in principle, S-BUN has the potential for scalability to different sizes, its diameter ( $d$ ) would directly impact its capacitive sensing performance. To determine the optimal size and scalability potential of S-BUN, we evaluated three different sensor diameters: 25 mm, 50 mm, and 100 mm (Fig. 5a). All sizes maintained the same hexagonal pattern (Fig. 3a) and features, differing only in size, enabling a direct comparison of capacitive sensing efficiency across different sizes.

Figure 5b reveals that the 50 mm S-BUN (medium) size provides an ideal balance between surface area and capacitive precision. This dimension ensures a robust capacitive sensing signal without compromising the compactness of the S-BUN module, making it suitable for robotic applications. Conversely, the 25 mm S-BUN (small) size, while advantageous for its compactness, exhibited a constrained capacitive sensing spectrum. This limitation diminishes its utility in applications requiring detailed touch differentiation due to its smaller surface area, narrowing the range of capacitive values. For the 100 mm S-BUN (large) size, while being capable of distinguishing between no touch, light touch, and hard touch, it encountered difficulties in distinguishing hover from other variations. This challenge arises from the overlapping capacitive values caused by its extensive surface area picking up noise from the environment, indicating a trade-off in capacitive clarity with increased S-BUN size.

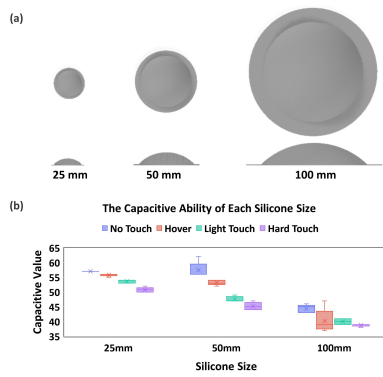


Fig. 5: Scalability of S-BUN. (a) Three tested sizes: 25mm, 50mm, and 100mm. Each retains the same features and hexagonal pattern dimension, with the only variation being the overall module size. (b) A graph illustrates the capacitive sensing capabilities of all sizes under various conditions: no touch, hover, light touch (pressed for 1 newton using a force gauge), and hard touch (pressed for 5 newtons using a force gauge). It should be noted that for the test, all S-BUN sizes have the same thickness, with  $t = 1$  mm.

However, it is noteworthy that the large size retains the essential capability to identify basic operations (no touch, light touch, and hard touch), suggesting its applicability in scenarios where touch differentiation suffices without the need for detecting approaching objects (hover).

This investigation of the effect of S-BUN size on capacitive sensing performance identified a scalability-trade-off dynamic. While the S-BUN size can be scaled, it affects capacitive sensing clarity, especially for hover interactions. Scalability in this context means that S-BUN can scale in size to accommodate different robot sizes without compromising performance. It does not imply enhanced capabilities with increased size.

### C. Experiment 3: Different S-BUN Setups

Since conductive materials are commonly used for soft touch sensors [5], [6], [7], [8], Fig. 6a displays a list of conductive materials tested for S-BUN sensing. The examined materials were conductive carbon ink (Liquiwire), a mixture of carbon powder and water, a mixture of graphite powder and water, pure carbon powder, pure graphite powder, conductive gel for active electrodes (g.tech g-GAMMA Gel), and a saltwater (NaCl) solution. These materials were evaluated for suitability in terms of their sensing performance and cost-effectiveness.

Fig. 6b presents the cost of each material per S-BUN unit in USD, offering insight into the economic viability of each option. Fig. 6c presents the capacitive performance of each material, providing a comparative analysis under different conditions such as no touch, hover, light touch, and hard touch. As can be observed, the conductive carbon ink (I) showed stable capacitive responses and had a moderate cost. The carbon powder and water mixture (II), though affordable, exhibited overlapping values between light and hard touch conditions, likely due to uneven carbon distribution. The graphite powder and water mixture (III) exhibited a balance between its sensing performance across touch conditions and cost-effectiveness. Conversely, the pure carbon powder (IV),

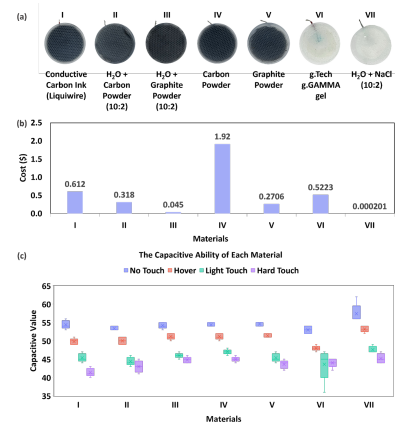


Fig. 6: Comparative analysis of different S-BUN setups with various conductive elements. (a) Examined conductive materials embedded within S-BUN with all other aspects remaining consistent except for the internal conductive material. The materials include (I) conductive carbon ink from Liquiwire, (II) a carbon powder and water mixture at a 10:2 (water-to-carbon) ratio, (III) a graphite powder sourced from pencils and water mixture at a 10:2 (water-to-graphite) ratio, (IV) pure carbon powder, (V) pure graphite powder, (VI) conductive gel for active electrodes from the g.tech, and (VII) a saltwater (NaCl) solution at a 10:2 (water-to-salt) ratio. It should be noted that the choice of the ratio was empirically set. (b) The cost (USD) of each material from (a) for a single S-BUN piece (3g). (c) The capacitive sensing capabilities from the conductive materials and their respective capacitive sensing under different conditions: no touch, hover, light touch (pressed for 1 newton using a force gauge), and hard touch (pressed for 5 newtons using a force gauge).

despite being the most expensive, did not demonstrate a significant performance improvement compared to the others. The pure graphite powder (V) encountered challenges in achieving uniform distribution within the silicone (observed during the experiment), thereby affecting its effectiveness. The g.tech g-GAMMA gel (VI) exhibited inconsistent results, particularly for light touches, despite its moderate cost. It also had trouble distinguishing between light and hard touches. Among all these, the saltwater solution (VII) stood out because it provided acceptable and consistent capacitive sensing in all conditions. It also provided the distinct (highest) no-touch value and outstanding cost-effectiveness.

Taken together, while each material presents unique advantages and limitations, the saltwater (NaCl) solution excels as the most balanced choice in terms of performance and cost. Due to its exceptional cost-effectiveness, along with consistent performance metrics, it is a suitable candidate for S-BUN sensing, ensuring reliable functionality and offering low-cost benefits for practical use in soft robotics.

### D. Experiment 4: S-BUN Application

To demonstrate the application of S-BUN for robot behavioral control and human-robot interaction, we implemented it on the pipe crawling robot iCrawl [1], where S-BUN served as the soft bifunctional utility module for the sensing and signaling of iCrawl (see [www.manoonpong.com/SBUN/video.mp4](http://www.manoonpong.com/SBUN/video.mp4)). This implementation involved placing two soft modules (S1 and S2, Fig. 7a)

of S-BUN, one on each leg of iCrawl<sup>3</sup>.

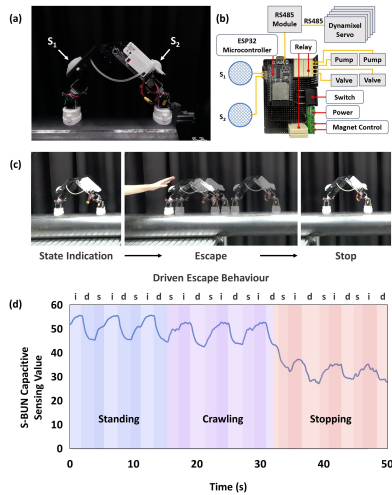


Fig. 7: The S-BUN setup on the iCrawl robot for robot behavioral control and human-robot interaction. (a) Two S-BUN soft modules (S1 and S2) on iCrawl. (b) Integrated S-BUN and iCrawl system overview. S1 and S2 indicate the S-BUN soft modules, each of which is controlled by one pump and valve. (c) S-BUN-driven escape behavior of iCrawl. When S-BUN senses an approaching human hand, it starts to crawl away from the hand to a safe distance. (d) S-BUN capacitive sensing values with the breathing function activated during different iCrawl states (i.e., standing still, crawling, and stopping states). i indicates the inflation phase of S-BUN, d indicates the deflation phase of S-BUN, and s indicates the stop or stabilization phase of S-BUN (see also Fig. 4).

Fig. 7b presents a system overview of the circuit board integrating the S-BUN and iCrawl systems. The S-BUN signal processing (low-pass filter) and iCrawl control (state machine) were implemented on the microcontroller ESP32 of the circuit board. The microcontroller transmitted the iCrawl control outputs (motor commands) to the iCrawl servo motors via an RS485 module (RS485 serial communication) and to the electromagnetic feet via magnet control channels.

The integration of S-BUN into the iCrawl enhanced the robot's signaling and sensing capacity for human-robot interaction. As depicted in Fig. 7c, initially, the robot was powered on and remained stationary (standing still) while S-BUN performed breathing to indicate the robot being in operation mode (robot state indication). When the robot detected an approaching human hand, it reacted by performing escape behavior (crawling in the opposite direction to maintain a safe distance, thereby avoiding being caught). Once the hand was no longer detected, the robot stopped crawling and resumed its stationary position. Furthermore, in situations where the robot experienced direct contact (S-BUN being touched), it was designed to immediately stop all operations

<sup>3</sup>The robot has two legs linked by one active body joint for unidirectional crawling. In total, it has five degrees of freedom (DOFs), with two DOFs for each leg and one DOF for the active body joint. Each DOF is driven by a Dynamixel XM430-W350-R servo motor. Additionally, each leg is equipped with an electromagnet foot for metal pipe surface adhesion. The robot's body measures 56 cm in length and 4 cm in width. It has a weight of 1.53 kg. The robot pipe crawling gait is generated by a state-machine based controller with IMU and hall sensor feedback, see [1] for further details on iCrawl.

as a protective measure<sup>3</sup>, preventing potential damage to its body and motor components.

During each phase of iCrawl's behavior, the S-BUN capacitive sensing signal constantly changed, as depicted in Fig. 7d. The S-BUN (S1) signal exhibited a rhythmic pattern while the breathing function was active. In the absence of any detected object, the rhythmic pattern oscillated between a high value of 55 during inflation and a lower value of 45 during deflation. However, upon detecting an approaching object, such as a hand, the pattern consistently decreased to a lower range between 52 and 42 throughout the breathing cycle. This change in pattern triggered the robot's escape crawling behavior. When a touch was detected, the pattern decreased further to a range between 35 and 26, varying with the phase of the breathing cycle and the touch pressure. In such cases, the robot responded by coming to a complete stop. It should be noted that we applied a simple moving average low-pass filter to obtain a smooth S-BUN signal for robot control and a threshold mechanism to switch between robot behavioral modes. The experimental results suggest that incorporating S-BUN into a robot could significantly enhance robot perception and safety during human-robot interaction.

#### IV. DISCUSSION AND CONCLUSION

The field of robotic perception has undergone a significant transformation with the advent of soft sensors, which offer a more sophisticated and nuanced approach to interaction with the environment. Our research on the Soft Bifunctional Utility Module for Robot Sensing and Signaling (S-BUN) represents a contribution to this evolving landscape. The module's design, drawing inspiration from the natural hexagonal pattern found in honeycombs, not only adds an aesthetic dimension but also confers structural benefits, particularly in terms of stress distribution. This choice of a bio-inspired design underscores the broader potential of nature as a source of inspiration for addressing contemporary engineering challenges.

By using a holistic approach, our work with S-BUN addresses research gaps in terms of high cost, complexity, single-function limitations, and the lack of versatility and adaptability/scalability of soft sensors. The module excels in mechanical resilience, thanks to its hexagonal pattern [18], [19], [20], and demonstrates superior capacitive sensing capabilities. It also has a signaling mechanism based on bio-inspired breathing for nonverbal human-robot communication [16]. The dual sensing and signaling functions of S-BUN set it apart from existing sensor designs. Nonetheless, comprehensive assessments of the system's durability, with and without hexagonal structures, as well as its lifespan under repeated use, are essential for future development and require further investigation. Additionally, variations observed in Fig. 6 highlight the need for more consistent and reliable proximity sensing values. Potential methods to improve consistency include optimizing the distribution and mixture ratios of conductive materials within the S-BUN module and employing signal processing techniques

to minimize environmental noise and enhance signal clarity.

A notable aspect of our development is the consideration of environmental sustainability in material selection. The use of a water and salt mixture, chosen for its impressive performance metrics, represents an environmentally friendly approach compared to traditional chemical-based sensors. This choice not only aligns with the growing need for sustainable practices in technology development [21] but also demonstrates the feasibility of using simple, non-toxic materials in advanced applications. However, it is important to acknowledge that while the saltwater component is environmentally benign, the silicone part of the sensor may not be as eco-friendly. This dichotomy presents an area for future research, with the aim of enhancing the overall environmental sustainability of the module. Alongside these environmental considerations, further research is necessary to address concerns regarding the S-BUN module's long-term resilience and adaptation in a variety of settings. These aspects of our research open up new avenues for future studies, particularly in the realm of material science within soft robotics, where the balance between performance, sustainability, and adaptability is crucial.

Our practical application of the S-BUN module on the iCrawl robot demonstrates insights into its real-world performance. While these experimental results show promise, further tests of the module's effectiveness are required to assess its adaptability and compatibility across a diverse range of robotic systems, including soft robots.

In conclusion, the research on the S-BUN highlights the potential of soft sensors in robotic perception system. The module's bio-inspired design, mechanical resilience, and dual sensing and signaling functions set it apart from existing sensor designs. Additionally, the environmentally friendly material selection and practical application of the iCrawl robot demonstrate the module's potential for real-world performance. However, further research is needed to address long-term resilience, adaptability, and compatibility across different robotic platforms. Additionally, exploring the integration of S-BUN in soft robotics is a promising area for future research to fully illustrate its benefits.

## ACKNOWLEDGMENTS

This research was supported by the BrainBot project (I22POM-INT010) of Vidyasirimedhi Institute of Science Technology (VISTEC) and the Marie Skłodowska-Curie Actions-Doctoral Networks (Grant Number 101119614, MAESTRI).

## REFERENCES

- [1] M. B. Khan, T. Chuthong, C. Danh Do, M. Thor, P. Billeschou, J. C. Larsen, and P. Manoonpong, "iCrawl: An inchworm-inspired crawling robot," *IEEE Access*, vol. 8, pp. 200655–200668, 2020.
- [2] A. H. Anwer, N. Khan, M. Z. Ansari, S.-S. Baek, H. Yi, S. Kim, S. M. Noh, and C. Jeong, "Recent advances in touch sensors for flexible wearable devices," *Sensors*, vol. 22, no. 12, p. 4460, 2022.
- [3] D. Rus and M. T. Tolley, "Design, fabrication and control of soft robots," *Nature*, vol. 521, no. 7553, pp. 467–475, 2015.
- [4] Y. Luo, S. Li, and D. Li, "Intelligent perception system of robot visual servo for complex industrial environment," *Sensors*, vol. 20, no. 24, p. 7121, 2020. [Online]. Available: <https://www.mdpi.com/1424-8220/20/24/7121>
- [5] G. Volpes, S. Valenti, H. Zafar, R. Pernice, and G. M. Stojanović, "Feasibility of conductive embroidered threads for i2c sensors in microcontroller-based wearable electronics," *Flexible and Printed Electronics*, vol. 8, no. 1, p. 015016, 2023. [Online]. Available: <https://iopscience.iop.org/article/10.1088/2058-8585/acbbdc>
- [6] C. Li, S. Yang, Y. Guo, H. Huang, H. Chen, X. Zuo, Z. Fan, H. Liang, and L. Pan, "Flexible, multi-functional sensor based on all-carbon sensing medium with low coupling for ultrahigh-performance strain, temperature and humidity sensing," *Chemical Engineering Journal*, vol. 426, p. 130364, 2021. [Online]. Available: <https://www.sciencedirect.com/science/article/pii/S1385894721019501>
- [7] A.-N. Kawde, N. Baig, and M. Sajid, "Graphite pencil electrodes as electrochemical sensors for environmental analysis: a review of features, developments, and applications," *RSC Adv.*, vol. 6, pp. 91325–91340, 2016. [Online]. Available: <http://dx.doi.org/10.1039/C6RA17466C>
- [8] X. Zhou and W. Cao, "Flexible and stretchable carbon-based sensors and actuators for soft robots," *Nanomaterials*, vol. 13, no. 2, p. 316, 2023. [Online]. Available: <https://www.mdpi.com/2079-4991/13/2/316>
- [9] S. Li, X. Xiao, J. Hu, M. Dong, Y. Zhang, R. Xu, X. Wang, and J. Islam, "Recent advances of carbon-based flexible strain sensors in physiological signal monitoring," *ACS Appl. Electron. Mater.*, vol. 2, no. 8, pp. 2282–2300, 2020.
- [10] J. Tulliani, B. Inserra, and D. Ziegler, "Carbon-based materials for humidity sensing: A short review," *Micromachines (Basel)*, vol. 10, no. 4, p. 232, 2019. [Online]. Available: <https://www.mdpi.com/2072-666X/10/4/232>
- [11] M. T. Almansoori, X. Li, and L. Zheng, "A brief review on e-skin and its multifunctional sensing applications," *Current Smart Materials*, vol. 4, no. 1, pp. 3–14, 2019.
- [12] B. Shih, D. Shah, J. Li, T. G. Thuruthel, Y.-L. Park, F. Iida, Z. Bao, R. Kramer-Bottiglio, and M. T. Tolley, "Electronic skins and machine learning for intelligent soft robots," *Science Robotics*, vol. 5, no. 41, p. eaaz9239, 2020.
- [13] J. Jørgensen, K. B. Bojesen, and E. Jochum, "Is a soft robot more 'natural'? Exploring the perception of soft robotics in human-robot interaction," *International Journal of Social Robotics*, pp. 1–19, 2022.
- [14] T. A. Klausen, U. Farhadi, E. Vlachos, and J. Jørgensen, "Signalling emotions with a breathing soft robot," in *2022 IEEE 5th International Conference on Soft Robotics (RoboSoft)*. IEEE, 2022, pp. 194–200.
- [15] B. Larsen, P. Manoonpong, and J. Jørgensen, "Wisard: Weight informing soft artificial robotic dermis," in *2022 IEEE 5th International Conference on Soft Robotics (RoboSoft)*. IEEE, 2022, pp. 1–8.
- [16] M. B. Christiansen, N. Asawalertsak, C. D. Do, W. Nantareekurn, A. Rafsanjani, P. Manoonpong, and J. Jørgensen, "Biomorf: A soft robotic skin to increase biomorphism and enable nonverbal communication," in *2023 32nd IEEE International Conference on Robot and Human Interactive Communication (RO-MAN)*. IEEE, 2023, pp. 370–377.
- [17] A. Asadi, O. Niebuhr, J. Jørgensen, and K. Fischer, "Inducing changes in breathing patterns using a soft robot," in *2022 17th ACM/IEEE International Conference on Human-Robot Interaction (HRI)*. IEEE, 2022, pp. 683–687.
- [18] C. Qi, F. Jiang, and S. Yang, "Advanced honeycomb designs for improving mechanical properties: A review," *Composites Part B: Engineering*, vol. 227, p. 109393, 2021. [Online]. Available: <https://www.sciencedirect.com/science/article/pii/S1359836821007642>
- [19] H. Mohammadi, Z. Ahmad, M. Petru, S. A. Mazlan, M. A. F. Johari, H. Hatami, and S. S. R. Kooloor, "An insight from nature: honeycomb pattern in advanced structural design for impact energy absorption," *Journal of Materials Research and Technology*, vol. 22, pp. 2862–2887, 2023. [Online]. Available: <https://www.sciencedirect.com/science/article/pii/S2238785422019524>
- [20] A. Nazir, A. B. Arshad, S.-C. Lin, and J.-Y. Jeng, "Mechanical performance of lightweight-designed honeycomb structures fabricated using multijet fusion additive manufacturing technology," *3D Printing and Additive Manufacturing*, vol. 9, no. 4, pp. 311–325, 2022. [Online]. Available: <https://doi.org/10.1089/3dp.2021.0004>
- [21] G. Giordano, S. P. Murali Babu, and B. Mazzolai, "Soft robotics towards sustainable development goals and climate actions," *Frontiers in Robotics and AI*, vol. 10, p. 1116005, 2023.